Geological Quarterly, 2000, **44** (4): 391–403

Development of fault pattern in the Silesian Nappe: Eastern Outer Carpathians, Poland

Jacek RUBINKIEWICZ

Rubinkiewicz J. (2000) — Development of fault pattern in the Silesian Nappe: Eastern Outer Carpathians, Poland. Geol. Quart., **44** (4): 391–403. Warszawa.

The development of fault pattern in the Silesian Nappe (Central Carpathian Depression) in the eastern part of Polish Outer Carpathians is outlined, from field observations and interpretation of air photos and radar images. Fault slip analysis and palaeostress reconstruction was applied to determine different systems of strike-slip, reverse and normal faults and the relative age of each system was determined. The results show a consistent evolution of fault systems which occurred as several episodes. Some of these episodes are local but others represent a regional pattern of faulting across the whole Polish Eastern Outer Carpathians. The beginning of fault evolution took place in Late Oligocene to Late Miocene times. The oldest phase is represented by reverse and thrust faults of system R_1 with SW–NE compression; a younger phase involves origination of strike-slip faults belonging to system S_1 (with the same direction of compression). Reverse (system R_2) and strike-slip (system S_2) faults were formed locally during a N–S compressional event. Dextral strike-slip faults of system S_3 with simultanous opening of a dextral set of fault system S_1 originated subsequently. The youngest events are represented by normal faults N_1, N_2, and N_3 systems during NW–SE, and SW–NE to N–S extension.

Jacek Rubinkiewicz, Institute of Geology, University of Warsaw, Żwirki i Wigury 93, PL-02-089 Warszawa, Poland; e-mail: rubik@geo.uw.edu.pl (received: May 18, 2000; accepted: August 18, 2000).

Key words: Polish Eastern Outer Carpathians, flysch, structural geology, fault slip analysis.

INTRODUCTION

This paper analyses fault pattern using mesostructural data collected from natural and artificial outcrops in order to reconstruct the structural evolution of the Silesian Nappe in its southeastern part in the Bieszczady Mts. (Fig. 1). It follows investigations on small-scale structures from the area (Rubinkiewicz, 1998).

The study area lies within one tectonic unit — the Central Carpathian Depression (Tołwiński, 1933) — comprising here the Oligocene-Miocene Krosno Formation (see Wdowiarz, 1985). Several sliced, thrusted one to another folds occur in the area. Recent investigations show that in most cases they are anticlinal forms with sloping, widely outcropping southwestern upper limbs. Outcrops of the steep, northeastern lower limbs are narrow and typically cut by large overthrusts (Fig. 1B), along which the anticlines are thrust over similar folds of the forefield. The regional fold axes and the stretching of the main thrusts are directed NW–SE in the part of the Silesian Nappe investigated (Książkiewicz, 1972).

Faults different in scale are common across the Outer Carpathians. Detailed analysis of fault pattern was carried out by Decker *et al.* (1997) in the western part of Polish Outer Carpathians, and this indicated polyphase faulting. Other papers describe faults from the Mszana Dolna tectonic window (Mastella, 1988) and the Babia Góra region (Aleksandrowski, 1989), which occur within the Magura Nappe. The structural evolution of the Romanian Carpathians, including its fault development, was described by Manteo and Bertotti (2000). No detailed structural analysis with stress field reconstruction has yet been carried out in this part of the Silesian Nappe. Regional papers (Opolski, 1930; Ślączka, 1968; Gucik *et al.*, 1980; Wdowiarz, 1980, 1985) present a generalised geological setting along with discussions on the main tectonic structures. The fault pattern has also been analysed from radar images (Mastella and Szynkaruk, 1999).

METHODOLOGY

The analysis is based on a new 1:25,000 geological map of the area (Rubinkiewicz, 1999). Faults were interpreted from air

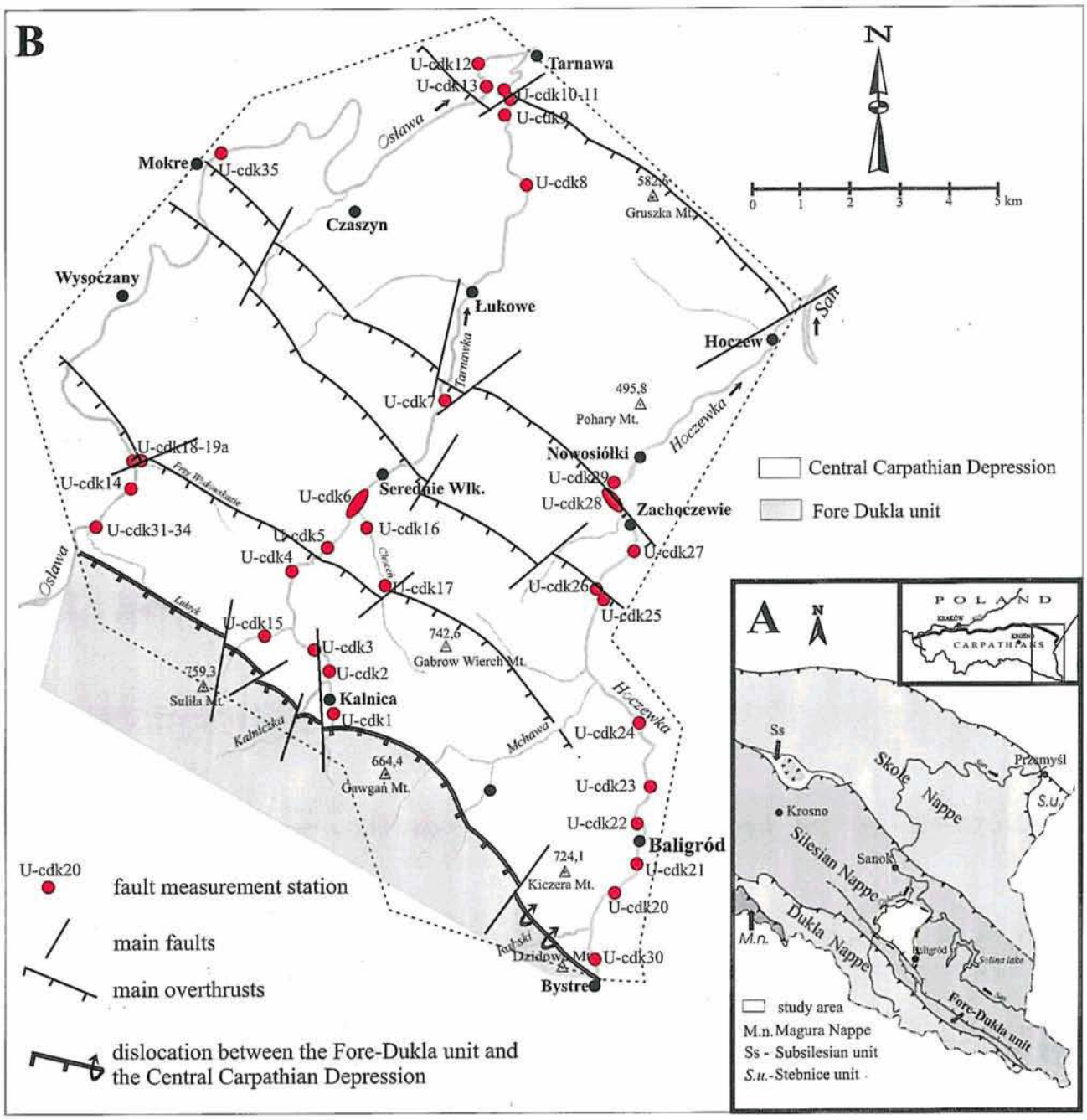

Fig. 1: A — Location map of study area; B — Location of the fault measurement stations with tectonic sketch

photos and radar images. Data collected in the field included that on faults visible at outcrop. Fracture cleavage, interbedded slips and series of *en echelon* fractures were interpreted separately. Initially, the field work comprised detailed observations at outcrop, including the lithology and orientation of bedding and fault planes, fault-related mineralisation and the magnitude, direction and sense of fault movement (Petit, 1987). Following Jaroszewski (1980, 1984) and Dadlez and Jaroszewski (1994), the following types of faults were distinguished: normal, strike-slip, reverse, oblique-slip, neoformed, reactivated, ductile and brittle, together with their relation to other structures (joints and minor folds) at outcrop. In cases of several generations of faults, their relative age as well as the probable conjugate relation of particular associations were determined.

The geometry of such fault displacements were first described by Anderson (1951). Numerical methods include those applied by Angelier (1979), Etchecopar (1981) or Reches (1987), while graphic methods were used by Arthaud (1969), Aleksandrowski (1985) and Lisle (1987) (see Angelier, 1994 for a full account of methods used in fault displacement analysis).

TectonicsFP software (Reiter and Acs, 1999) was used for structural data analysis, particularly of fault slip. The first phase of data processing included preparation of plots of fault slip

data from each outcrop and of the senses of displacement. The method of Angelier (1979), presenting the fault planes as great circles and the orientation of slickenlines in form of points with arrows showing the sense of slip of the upthrown block, was applied (Fig. 2). All diagrams are in a lower hemisphere projection. Selected diagrams are shown here to illustrate the particular systems and sets of faults.

The data sets, shown on particular diagrams from outcrops, are typically non-uniform (Fig. 2A), and so were subsequently separated into uniform sub-sets (Fig. 2B). The stress and strain fields, in which the systems and sets of faults were generated, were then analysed. In the case of sets of conjugate faults, the value of the shear angle Θ and orientation of the principal stress axes σ_1, σ_2, σ_3 were determined using the method of rectangular sectors (Dihedra, P-T axes — Turner, 1953), an inversion method (Angelier and Gougel, 1979; Sperner and Ratschbacher, 1993) as well as the numeric dynamic analysis method (NDA — Spang, 1972). Next, compression and extension directions were determined, along with their regional variability. Finally, stages of the development of particular fault sets and systems were determined and their relative age was interpreted.

Three main tectonic regimes of fault development (Fig. 3) differing in the orientation of the main stress axes ($\sigma_1 > \sigma_2 > \sigma_3$) are distinguished in the subsurface part of the Earth's crust (Anderson, 1951). The first is characterised by the development of reverse faults (σ_1 — horizontal, σ_3 — vertical), the second by the development of strike-slip faults (σ_1 and σ_3 — horizontal), and the third by normal faults (σ_1 — vertical, σ_3 — horizontal). Systems of oblique-slip faults are rare. The commonly used geometric subdivision of faults into diagonal, parallel and perpendicular in relation to the orientation of regional axes of folds and overthrusts was applied in the paper.

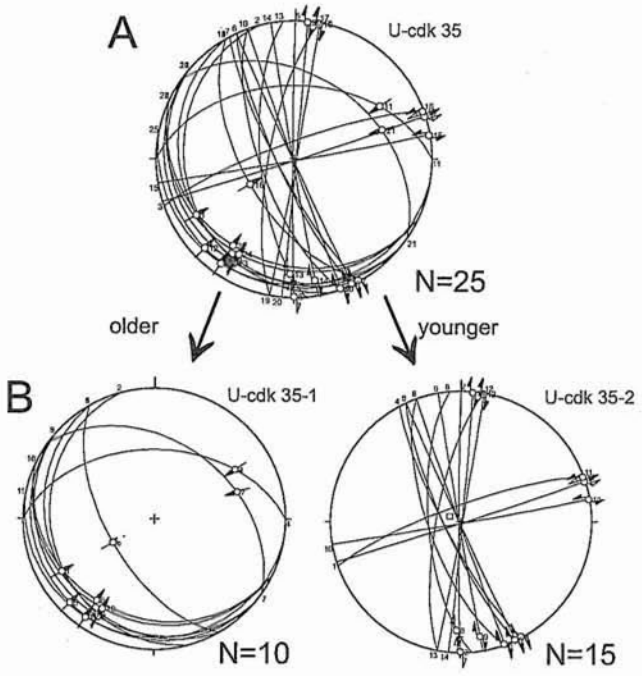

Fig. 2: A — Angelier plot illustrating fault slip data (equal area, lower hemisphere projection — used in the entire paper); B — Diagrams after manual sorting of fault slip data

Lower right corner of diagram — number of measurements, upper right corner of diagram — number of fault measurement stations

A total of 545 fault planes were measured, 52% of which included strike-slip faults, 25% reverse faults, 16% normal faults and 7% oblique-slip faults.

FAULTS

Data were collected in 35 outcrops evenly distributed in the investigated area (Fig. 1B). In most cases they include small faults with displacements not exceeding several metres. Large dislocation zones were observed in many outcrops, characterised by the occurrence of breccia and cataclasite zones up to several metres across as well as by strong folding of rocks directly adjacent to the fault zone. Analysis should be cautious in these zones, as many of the small-scale faults occurring there are of a second order in relation to the main dislocation. Abrupt changes of strike resulting from drag folds testify to the close presence of the fault zone.

Most outcrops with faults occur within relatively ductile shale and shale-sandstone units (by comparison with units of thick-bedded sandstones).

The direction and sense of the fault displacement was determined on the basis of structures present on the fault surface or in its direct neighbourhood. Typically these included slickensides with calcite coats with distinct steps and slickenlines. Occurrence of other structures depends on the type of fault and is described below.

STRIKE-SLIP FAULTS (S)

Strike-slip faults, that is faults with max. 10° deflection of slickenlines from the horizontal, prevail among small faults observed in outcrops. Although strike-slip faults are observed in different tectonic situations and in different parts of the Krosno beds, their outcrops are concentrated mainly within overthrust zones (Fig. 4).

Beside slickensides, the direction and sense of slip of strike-slip faults were determined on the basis of drag folds (Fig. 5A and 6A) and folds with vertical axes, and in brittle rocks, i.e. sandstones, on the basis of low-angle Riedel shears, situated at about 20° in relation to the main fault plane (Fig. 5B). In zones of larger faults, small shears, situated *ca.* 20–35° in relation to the strike of the main fault zone, were often observed, which comprise typical feather fractures (Dadlez and Jaroszewski, 1994). Small contractional strike-slip duplexes were common in ductile beds, while comparable extentional structures occurring in more brittlle sandstone units were most rarely observed (Fig. 5C, D). All these structures can be observed along single fault zones, and their occurrence depends on the lithology of rocks and on local deformation conditions.

The observed length of strike-slip faults is variable. The longest can be traced for several hundreds of metres, based on analysis of air photos and radar images, while their wide deformation zones, breccia and cataclasites are present in outcrops

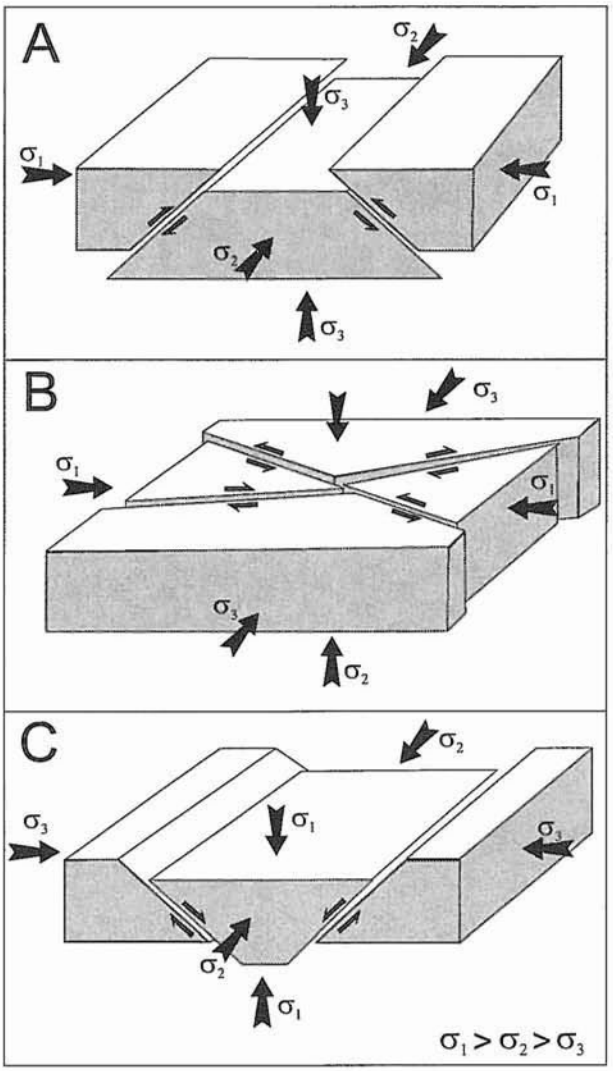

Fig. 3. Tectonic regimes in relation to fault systems: **A** — compression — reverse faults, **B** — compression — strike-slip faults, **C** — extension — normal faults

within streams. The length of strike-slip faults observed in outcrops does not exceed a dozen or so metres, typically several metres. Faults often lie en echelon, supplying additional criteria for determining the sense of displacement.

The scale of horizontal displacement of strike-slip faults observed in outcrops varies from a dozen or so centimetres (Figs. 5, 6) to 1 m. Larger displacements can be deduced from lithological contrasts in both walls, and in the case of faults interpreted from radar images (archive of Polish Geological Institute) this displacement may reach several hundred metres.

Planes of strike-slip faults are typically vertical or very steep (dip 70–90°). Some faults disappear in beds of ductile shales (Fig. 6A). Faults disappearing on non-ductile bed surfaces (Fig. 6B) as well as transitional to interbedded slip in cases of acute angles between fault and bed strike (Fig. 6C) have also been observed. Occasionally, secondary, often mineralised fractures or accompanying faults occur at ends of faults (Fig. 6D).

Two sets of diagonally intersecting strike-slip sets with opposing senses of displacement (dextral and sinistral) can often be observed in individual outcrops. They compose a conjugate system, for which the magnitude of shear angle and the orientations of main stress axes can be determined.

Three systems of strike-slip faults have been distinguished in the area investigated.

SYSTEM S_1

Sets of faults diagonal in relation to the orientation of the main NW–SE structural direction have been observed in many outcrops, where the dextral set has an azimuth of 10–30° and the sinistral set an azimuth of 60–85°. Typically both sets occur in individual outcrops (Fig. 7A, C), however, in some cases, one of the sets dominates (Fig. 7B). The shear angle Θ value (Fig. 8), measured in exposures varies between 23 and 34° with values of 24 and 32° dominant, and does not depend on lithology. However, fault surfaces can often be curved (Fig. 6C), therefore values of this angle can vary slightly even within one exposure. Values obtained of the shear angle are similar to those previously noted (i.e. Dadlez and Jaroszewski, 1994, p. 72). In cases when the complementary set was lacking, the orientation of σ_1 stress was tentatively reconstructed on the basis of shear angle Θ value. For this system the axis of the σ_1 stress has the azimuths of 15° (SSW–NNE) and 46° (SW–NE).

Typically the dextral set is more mineralised. Secondary calcite overgrowths with well developed drusy crystals occur there. The increased migration of hydrothermal solutions could result from wider opening of fissures of this fault set, which in turn suggests extensional conditions in the later phase of their development linked with the formation of system S_3.

Faults of this system, occurring in shale-dominated units, do not use earlier discontinuity surfaces and attenuated zones in rocks, and so can be treated as neoformed faults. Sporadic reactivated slides were observed in thick- and medium-bedded sandstones diagonal joint planes (Rubinkiewicz, 1998), the orientation of which is similar to the orientation of the diagonal fault sets.

The analysed sets cut folds and overthrusts as well as the observed small-scale reversed faults, as inferred from analysis of intersection relations in the field and on maps, thus they are obviously younger than the phase of development of the main tectonic structures in the region. The pattern of orientation of small-scale faults representing this system is identical with the pattern of large faults interpreted from radar images (Fig. 9), as well as with the interpretation of Mastella and Szynkaruk (1999) for this region. System S_1 resulted from SW–NE and SSW–NNE compression (tectonic shortening).

SYSTEM S_2

In the southern part of the area near Kalnica (Fig. 4) a local change in the axes of regional structures to longitudinal is observed. This takes place in the Fore-Dukla zone as well as in the Central Carpathian Depression near the overthrust separating the two units. Sets of conjugate faults occur here, intersecting

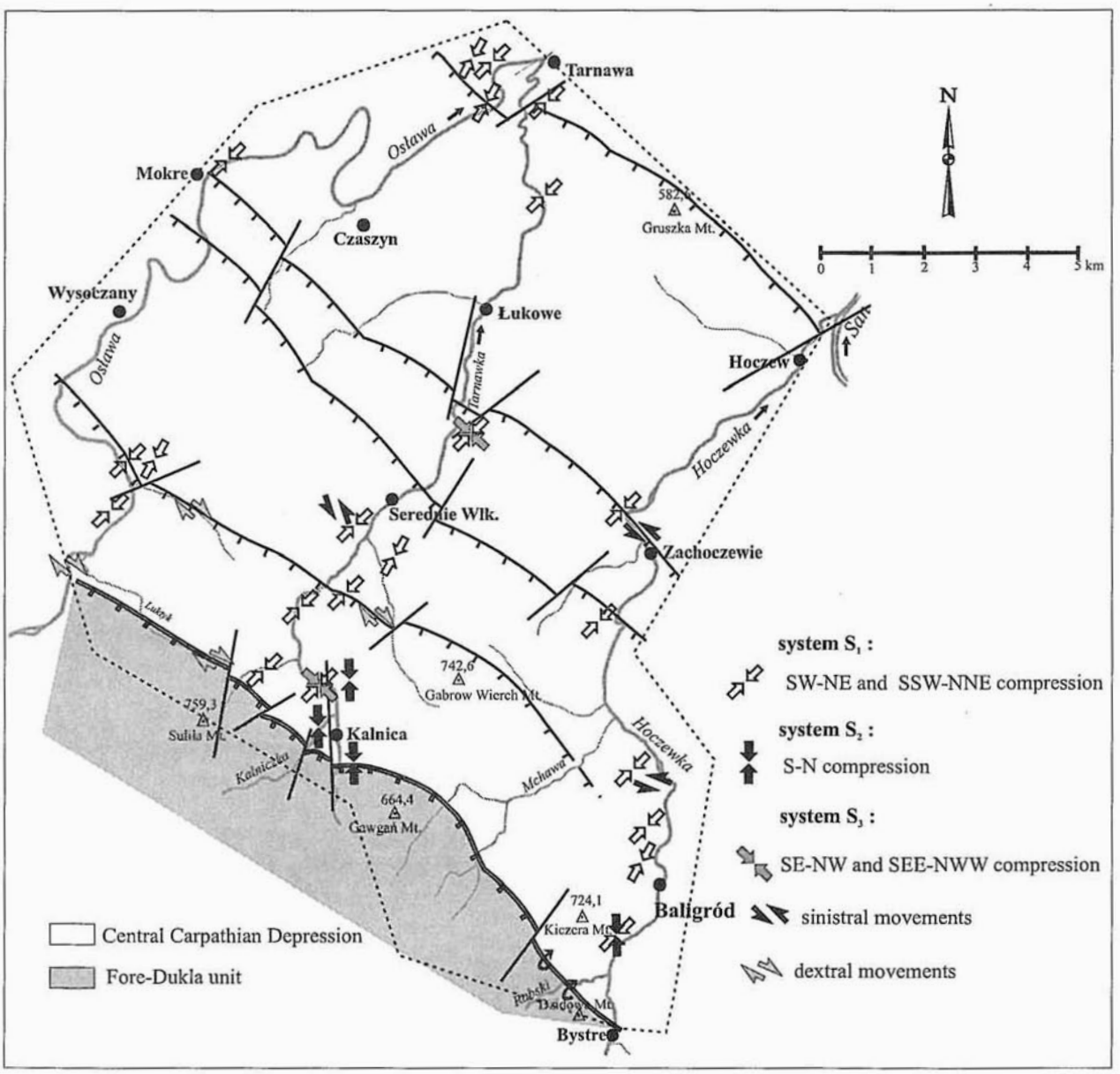

Fig. 4. Main directions of compression and strike-slip movements inferred from strike-slip faults

For other explanations see Fig. 1

each other at *ca.* 60°, oriented differently to those of system S_1. Sinistral faults are oriented at an average of 20–45°, and dextral faults at 140–160°. This resulted from their development in a stress field characterised by σ_1 orientation and an azimuth of 0° (Fig. 7C).

Reactivation of dextral faults of system S_1 by sinistral faults of system S_2 is observed in some outcrops. This development can be linked with a local change of the structural pattern, probably caused by a change in the direction of overthrusting of the Fore-Dukla unit. This took place later than the formation of the main tectonic structures in the area, as well as after the dominant S_1 system of diagonal faults. This system developed during N–S compression.

SYSTEM S_3

Sets of longitudinal dextral (dominant) and locally sinistral strike-slip faults, parallel to, or at low angles to, the orientation of the regional structures in the area have been observed south of the Mokre–Zachoczewie line (Fig. 4), typically in overthrust zones. Strikes of fault surfaces vary between 90 and 145°, with a prevalence of faults with a strike of 130°. In some outcrops both sets are present, and the Θ angle of this pair is smaller (Fig. 7D) than in the case of diagonal faults and varies between 17 and 25°. This suggests their formation in a stress field with an increased role of extension (analogous with hybrid shears — Hancock, 1985), which was probably caused by more brittle failure in low pressure conditions.

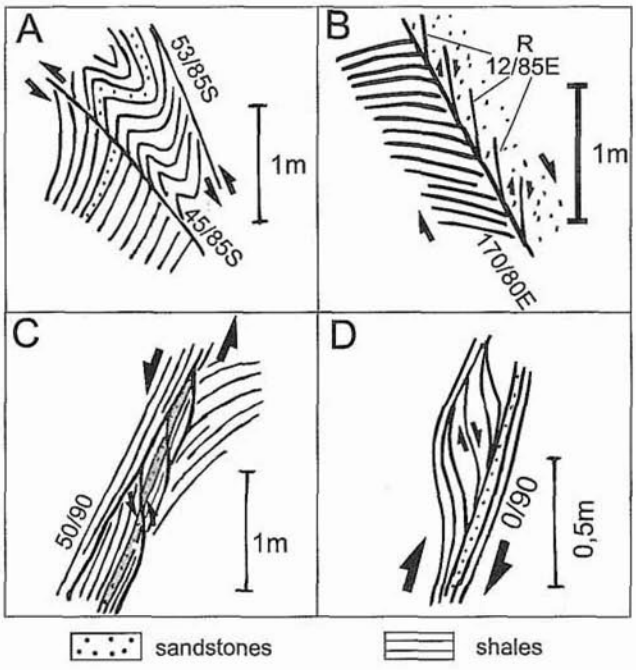

Fig. 5. Examples of structures for determining sense of slip for strike-slip faults (map view): **A** — drag folds with steeply dipping axes, **B** — Riedel shears (R), **C** — extensional duplexes, **D** — contractional duplexes

Fault surfaces are not always vertical; in some cases they dip at 45–70° to the NE and SW. This is caused by displacement taking place along earlier reversed fault surfaces, thus these are reactivated faults.

The observed temporal succession suggests that they formed after the faults of systems S_1 and S_2. Their development is linked with indefinite strike-slip movements generally taking place along overthrusts.

REVERSE FAULTS (R)

Outcrops with reverse small-scale faults are concentrated in overthrust zones and their neighbourhood (Fig. 10). This group comprises reverse faults with displacement angles not exceeding 20° to the dip.

The direction and sense of displacement for reverse faults was determined on the basis of tectoglyphs on slickenside surfaces and the drag folds. The vergence and geometry of folds near overthrusts were also analysed (Fig. 11A, B). Shale-rich units yield folds characterised by a variable parallel and disharmonic geometry (Fig. 11A), while non-ductile beds are folded in larger, more concentric forms. In both cases the direction perpendicular to the fold axis represents the direction of displacement, and the vergency of folds is its sense.

Typically small parts of the reverse fault planes or small overthrusts are present in outcrops. Small-scale reverse faults, truncating the beds and disappearing in the surrounding shales, are present in steeply inclined sandstone beds, while the sloping sandstone beds lack shears, which pass into flexural slips.

In the analysed group of small-scale faults the displacement varies between several to over a dozen metres. In some cases the fault gets steeper (Fig. 11A, B). Thus the dip angles of fault planes reveal a considerable variety, although fault sets with dips between 20 and 55° southwards dominate (Fig. 12). Steeping of reverse fault planes towards the surface may indicate the existence of overthrusts forming imbricate structures (see Mastella, 1988; Dadlez and Jaroszewski, 1994), originating due to branching of secondary overthrusts from a sloping decollement surface.

The disappearance of such faults typically results either from gradual steeping of the fault surface, branching into secondary faults (Fig. 11A) or from the formation of a fold over the end of the fault (Fig. 11B), referred to as the fault propagation fold.

Sets of conjugate reverse faults were determined and measured only in some outcrops (i.e. Fig. 11C) therefore the orientation of the axes of the marginal main stresses can be determined approximately. The Θ angle values vary between 20 and 40°, very often attaining different values even within one exposure, which results from the earlier steepening of fault planes described above.

Two systems of a regular structural pattern formed by small reverse faults can be distinguished on the basis of the data collected.

SYSTEM R_1

Longitudinal faults with strikes parallel to the direction of regional structures in the area (azimuth 110–130°) and SW dips prevail in the exposures. Sets of small-scale reverse overthrusts with NE dips are rare (Fig. 11C). In some cases sloping overthrust surfaces with variable S and N dips were observed within one outcrop (Fig. 12C). This often points to the existence of sloping normal and reverse faults, typical for one slip surface or for the occurrence of R and P shears (Dadlez and

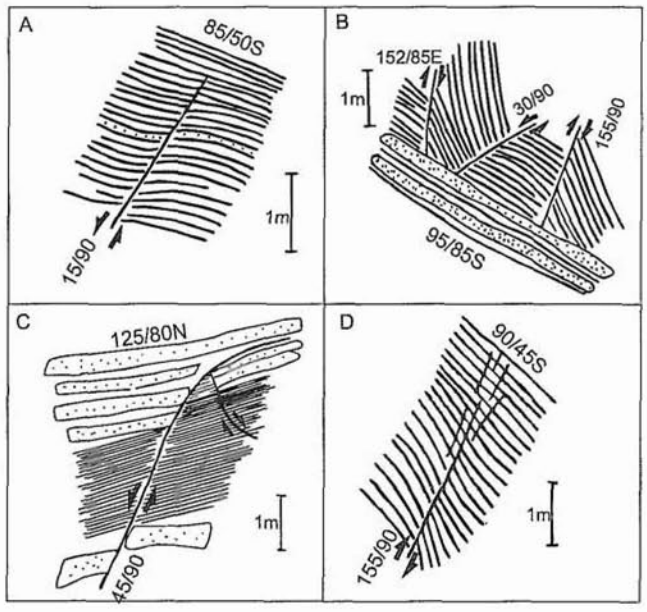

Fig. 6. Examples of strike-slip fault accomodation (map view): **A** — disappearance in shales, **B** — disappearance on neutral surface, **C** — transition to interbedded slip, **D** — secondary fractures at the end of fault

Jaroszewski, 1994, p. 84), accompanying the main dislocation. Practically all observed reverse faults are mineralised with calcite. The system originated during SW–NE and SSW–NNE compression (Fig. 10).

Faults of this system originated after the formation of the main regional folds, when further tectonic shortening due to folding from bending was no longer possible. This is suggested by the identical orientation of overthrusts and reverse faults in upper and lower limbs of regional folds.

SYSTEM R_2

Locally (Fig. 10), near the overthrust of the Fore-Dukla unit near Kalnica (see system S_2), a set of reverse faults with strikes between 75 and 110° and southern dips was observed. In places its conjugate equivalent with similar strikes and with northern dips co-occurs. System R_2 is distinguished only in this area, and so its formation is probably connected with a local W–E trend in the course of regional structures. The faults are cut by strike-slip faults of system S_2; they are thus older, although they also developed due to N–S compression (Fig. 12A), although with a different orientation of the principal stress axes.

The observed systems of reverse faults are mainly neoformed faults. In later phases their planes were reactivated as strike-slip or normal faults.

NORMAL FAULTS (N)

This group includes faults distinguished on similar criteria of displacement direction as reverse faults, however with an opposite sense. Small-scale normal faults are much rarer than reverse faults. They typically occur with other generations of faults, particularly with reverse faults (Fig. 10).

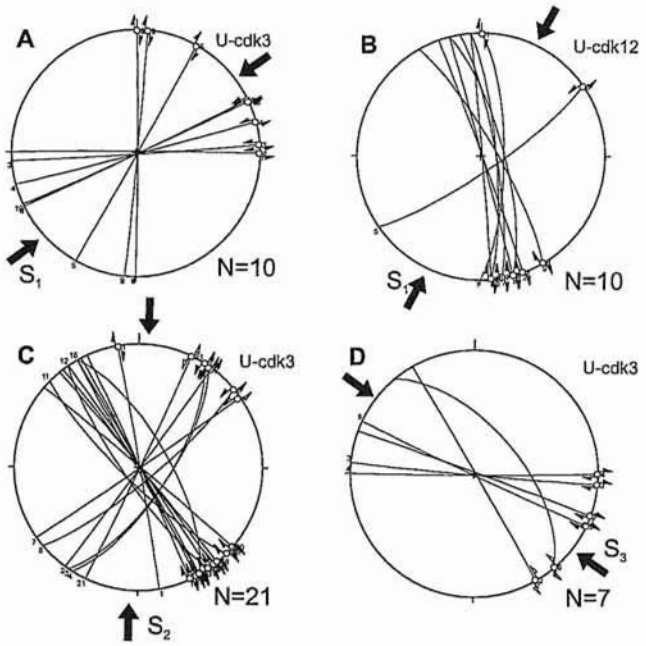

Fig. 7. Examples of diagrams of strike-slip faults: **A** — system S_1 of conjugate faults, formed during SW–NE compression, **B** — example of domination of one fault set, formed during SW–NE compression, **C** — system S_2 of conjugate faults, formed during local S–N compression, **D** — system S_3 of conjugate faults, fomed during NW–SE compression with predominant dextral faults

For other explanations see Fig. 2

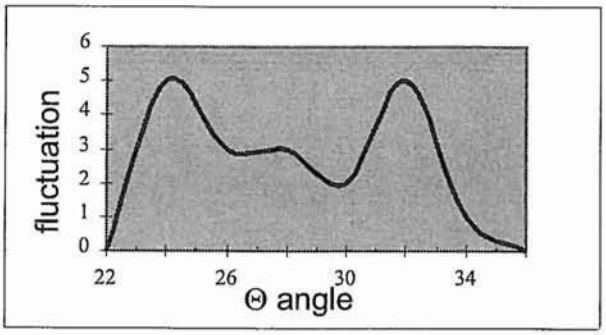

Fig. 8. Fluctuation graph of Θ angle for system S_1 of conjugate strike-slip faults

The senses and directions of the displacements were typically determined on the basis of drag folds (Fig. 11D), low angle Riedel shears (Fig. 11E) and the displacement of strata in both fault sides.

The displacement of the normal faults investigated varies from several centimetres to several metres. Cataclasites and breccia (Fig. 11F) accompany some faults, which may form *en echelon* arrays.

In some outcrops, normal faults occur in two sets with opposite senses (Fig. 11E), forming a conjugate system. Their mutual disappearance is observed on surfaces of the complementary set. Minor calcite mineralisation occurs along these faults.

A great variety is observed in the angles of dip of the normal fault planes, from vertical or very steep (dip angles 50–90°) to gently sloping (dip angles 15–45°). This results from their shovel shape, causing dip to vary even within one exposure.

The pattern of normal faults is complicated in comparison with other systems, comprising at least three systems of faults, which can co-occur within one outcrop (Fig. 10 — Osława river).

SYSTEM N_1

The first group includes sets of transverse faults, locally diagonal in relation to the orientation of axes of the regional structures (Fig. 12D), with strikes of 20–60° and steep dips of 50–90° towards the NW and SE, forming a conjugate system. Their exposures are concentrated in the southwestern part of the area (Fig. 10). These faults also intersect reverse faults of system R_1 and diagonal strike-slip faults of system S_1. They most probably represent the NW–SE extension phase. Some of the faults are neoformed, while a part of them reactivates earlier planes of diagonal strike-slip faults of system S_1.

SYSTEM N_2

The second system, evenly distributed on the investigated area (Fig. 10) comprises longitudinal normal faults characterised by a mean strike of 110–140°. One or two systems (Fig. 12E) of conjugate faults occur, characterised by variable dips towards the NE and SW. In most cases they include reactivated

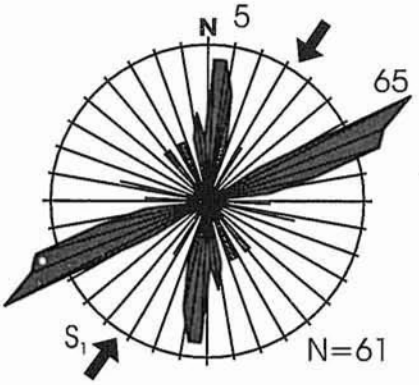

Fig. 9. Rose diagram of strike-slip faults interpreted from radar images

faults, using surfaces of longitudinal reverse faults, and so they often dip at low angles (Fig. 12E). Very steeply dipping sets tend to be neoformed, cutting reverse faults of system R_1 and diagonal strike-slip faults of system S_1. Therefore this system formed in a younger phase of SW–NE extension.

SYSTEM N_3

This group comprises sets of diagonal faults with strikes of 80–100° and typically low-angle dips of 10–35° towards the N and S. Their occurrence in the area is completely random (Fig. 10). Similarly to the previous ones, they are younger than the reverse and strike-slip faults, and formed during N–S, or in some cases NNE–SSW extension.

Intersecting relations show that these normal faults are younger than strike-slip and reverse faults. None of these groups of faults dominates. According to Reches (1983), a subsequent development of discontinuous structures with a different deformation direction (i.e. variable σ_3 orientation, constant σ_1 orientation) can take place in a triaxial stress field. Thus, faults of systems N_2 and N_3 may have originated during one deformation phase.

OBLIQUE-SLIP FAULTS

Faults of this group comprise only a small part of the faults measured in outcrops. They are characterised by a variable orientation and do not form uniform sets. "Reverse" and "normal" faults were observed in this group.

Two cases of the occurrence of these faults are worth mentioning. The continuous change of line orientation within one fault plane may indicate a gradual change of direction of relative block movement (see Jaroszewski, 1968), caused by unknown local factors. In the second case, oblique-slip faults, which after retrodeformation against bedding position turn out to be normal faults, have been observed in the youngest part of the Krosno beds. A variable thickness of the same beds was observed along both sides of the fault, as well as variable slip, indicating that the faults might be synsedimentary, representing a pre-folding phase.

INTERPRETATION

The earliest pre-folding development phase is represented by synsedimentary faults observed in the youngest flysch members, locally dated as Early Miocene (Malata, pers. comm.), however due to insufficient data the directions of extension within the sedimentary basin have not been determined. Flysch sedimentation, which terminated in the Late Oligocene, was followed by folding (Ślączka, 1996), and this resulted in the development of regional folds.

During the initial folding phase, flysch masses were transported along large overthrusts with the simultaneous formation of NE verging regional folds. Secondary overthrusts developed from these large overthrusts (Fig. 13). They formed along the axial planes of synclines (Rubinkiewicz, 1999), cutting lower limbs of the regional anticlines and steepening towards the surface (Fig. 13). This led to the formation of an imbricate system (Fig. 13), typical of the tectonic pattern of this part of the Central Carpathian Depression. The formation of such structures depends on the lithology of the Krosno beds, composed largely of medium- and thick-bedded competent sandstones, thus leading to the formation of regular regional fold structures. More complicated tectonic deformations occur locally in shale-rich units and situated near various tectonic dislocations such as strike-slip faults.

Reverse faults and overthrusts of **system R_1** originated as secondary structures in zones of the steepening overthrust planes, as well as in their direct forefield. Analysis of the strain field from exposures points to their origination during SW–NE compression.

During the final phase, steepening of overthrusts caused termination of the slide and further tectonic shortening, which led to switch in orientation of the intermediate and the least principal stresses and the formation of diagonal strike-slip faults of **system S_1**, cutting overthrusts. They were formed during the same SW–NE compression. These fault systems are neoformed, though some of them may also have utilised earlier attenuated and failure planes in the flysch complex, i.e. from the phase of diagonal joint formation (Rubinkiewicz, 1998).

After the formation of these fault systems, a local change in the orientation in regional structures took place, caused most probably by a change in the thrusting direction of the Fore-Dukla unit. This resulted in the formation of overthrusts and reverse faults of **system R_2** in the vicinity of Kalnica (Fig. 4), followed by strike-slip faults of **system S_2**, of which some reactivated faults of **system S_1**. Both systems originated during local N–S compression.

The next phase is connected with the reactivation of overthrusts of **system R_1**. Longitudinal, usually dextral faults of **system S_3**, suggesting a phase of strike-slip movement along the planes of the main overthrusts, were observed along overthrusts of **system R_1** or in their direct vicinity. They were formed mainly in the southern part of the area investigated (Fig. 4). Opening of pre-existing fault fissures and secondary mineralisation of dextral faults of **system S_1** also took place during this phase, pointing thus to secondary extension during simple shearing (Fig. 14). Dominantly dextral movements of this type were noted e.g. at the boundary between the Magura and

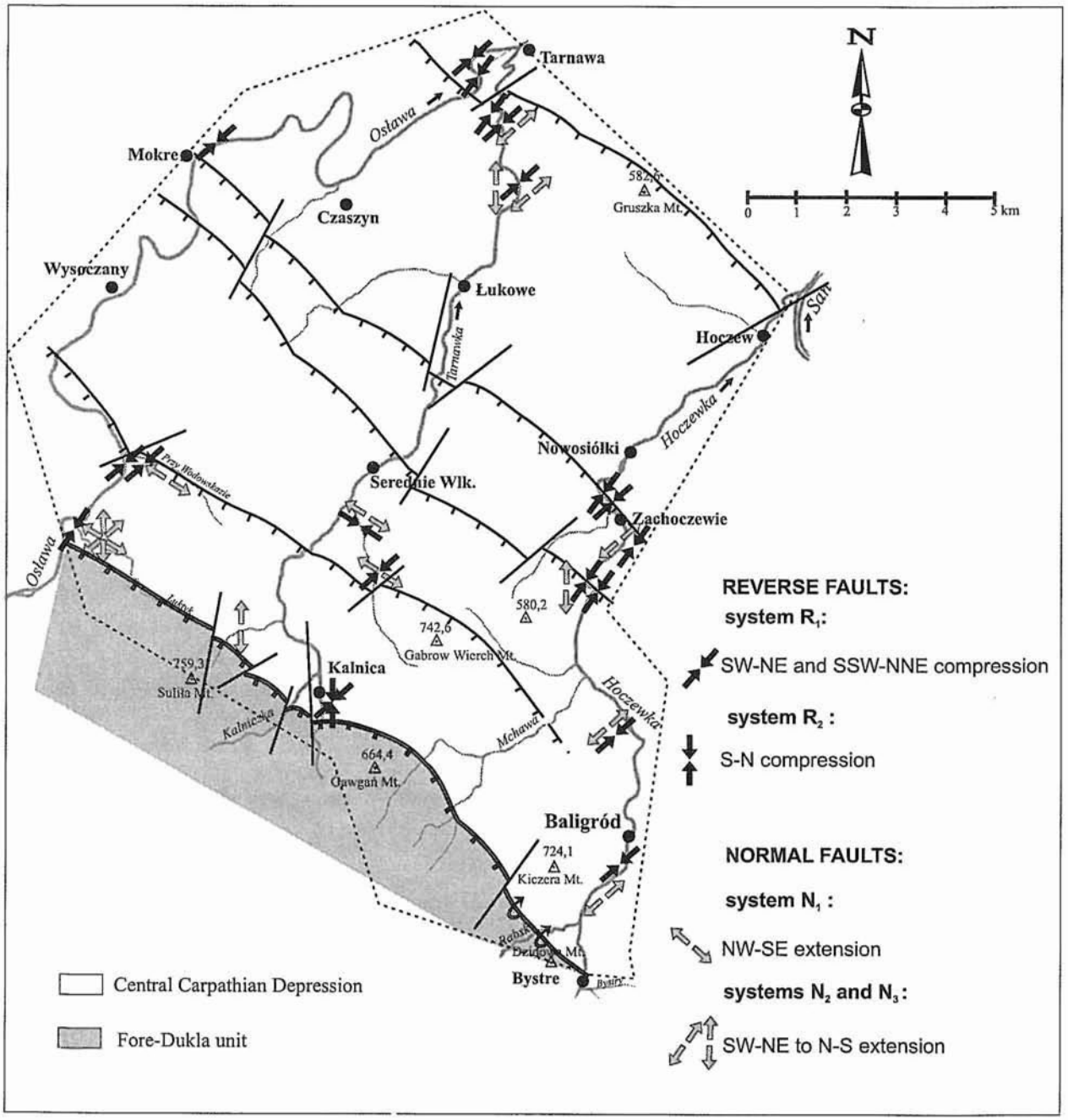

Fig. 10. Main directions of compression and extension inferred from reverse and normal faults

Silesian nappes (Decker *et al.*, 1999) and dated as post-Middle Miocene.

A decrease of horizontal compression during the initial phase of the post-orogenic heave of the Carpathians resulted in the possibility of stretching the flysch complex. Transverse normal faults of **system N_1** were formed in this phase (Fig. 14). They cut overthrusts of **system R_1** as well as strike-slip faults of **system S_2**, the latter being locally reactivated. This testifies for a younger phase of deformation linked with NW–SE extension, therefore parallel to the course of the regional structures. Faults of this system have been observed mainly in the southwestern part of the area investigated, where the tectonic deformation is most intense.

Most probably, the last, youngest phase of fault development took also place in the later phase of the post-orogenic heave of the Carpathians, however without horizontal compression. This resulted in the formation of longitudinal normal faults of **systems N_2** and **N_3**, which locally utilised planes of earlier reverse faults of **system R_1**. Additionally, steep neoformed faults originated.

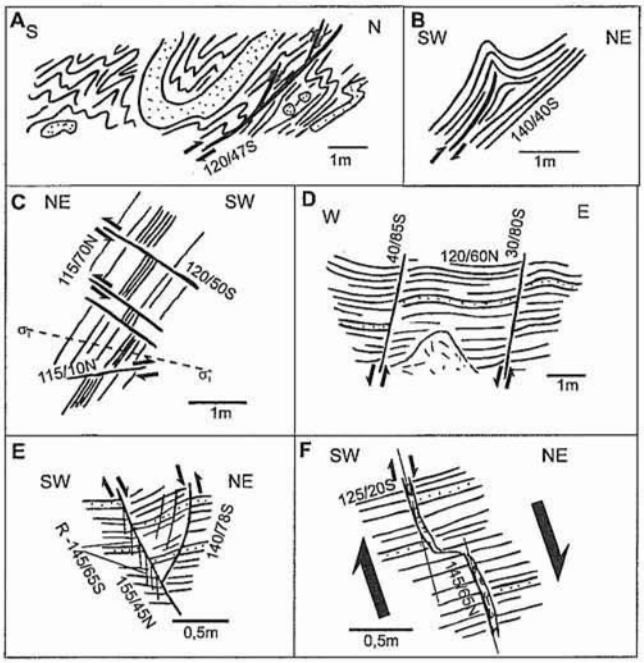

Fig. 11. Examples of outcrops with reverse (**A–C**) and normal (**D–F**) faults (cross-section): **A** — aboverthrust zone with secondary structures related to main overthrust, **B** — fault propagation fold, **C** — system of conjugate reverse faults, **D** — set of normal folds with drag structures, **E** — system of conjugate normal faults, **F** — *en echelon* array of normal faults

Two phases of calcite mineralisation of different age have been distinguished in the fault zones investigated. Earlier, syn-kinematic mineralisation is more common and took place during the formation of all fault types. Numerous slickensides originated then. Later, post-kinematic mineralisation formed secondary calcite overgrowths on fault planes, usually growing over earlier-formed slickensides. Such secondary mineralisation is present on planes of the dextral fault set of **system S_1**.

Zones of reverse faults are usually most mineralised, of strike-slip faults to a lesser degree, while zones of normal faults are typically least mineralised. This is probably due to deeper penetration of flysch masses by reverse and strike-slip faults, so the migration of hydrothermal solutions was facilitated. Such mineralisation may have taken place recently (Gruszczyński and Mastella, 1986), as testified to by the occurrence of travertines in zones of reverse faults.

CONCLUSIONS

The fault pattern in the investigated area of the Silesian Nappe comprises several systems and sets of faults. Each of them has a stable orientation in relation to the strike of the main tectonic structures, forming a generally uniform structural pattern. Some of the measured fault systems are observed across the whole area (e.g. system R_1 or S_1), while the others are local (i.e. R_2 or S_2). Therefore detailed analysis of small faults identified areas with a more or less complicated evolution of the fault pattern and the associated phases of compression and extension.

Analysis of the fault pattern in the investigated area of the Central Carpathian Depression has indicated several phases of fault development.

Regional SW–NE compression resulted in the development of the following fault systems (Fig. 14):

Phase I. Development of a set of reverse overthrusts and faults (**system R_1**), forming an imbricate structure, cutting regional folds, in a stress field characterised by σ_1, σ_2 — horizontal, σ_3 — vertical during the terminal folding phase.

Phase II. Formation of diagonal strike-slip faults (**system S_1**), cutting folds and overthrusts in a stress field characterised by σ_1, σ_3 — horizontal, σ_2 — vertical.

Change of compression into N–S (Fig.15) resulted in the local reorientation of regional structural directions, causing the following phases to develop:

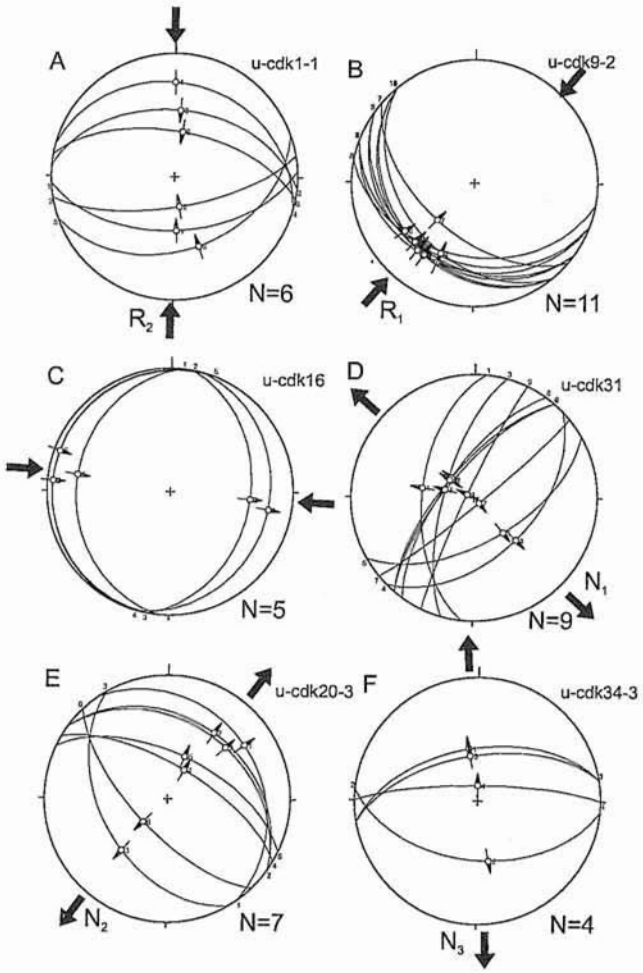

Fig. 12. Examples of diagrams of reverse (**A–C**) and normal (**D–F**) fault data sets: **A** — system R_2 of conjugate reverse faults, formed during local N–S compression, **B** — one set of reverse faults (system R_1), formed during SW–NE compression, **C** — example of subhorizontal thrust surface, **D** — system N_1 of steeply dipping normal faults, formed during SE–NW extension, **E** — system N_2 of normal faults, formed during SW–NE extension, **F** — system N_3 of normal faults, formed during N–S extension

For other explanations see Fig. 2

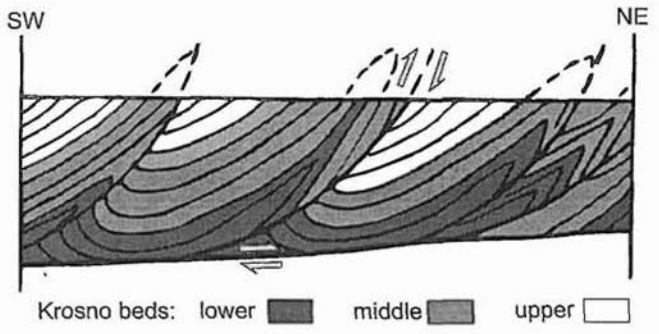

Fig. 13. Schematic cross-section through the investigated area showing the geometry of main (regional) folds and overthrust

Phase IIIa. Overthrusts and reverse faults of **system R_2** in a stress field characterised by σ_1, σ_2 — horizontal, σ_3 — vertical.

Phase IIIb. Strike-slip faults of **system S_2**, locally reactivating dextral faults of system S_1 ($IIIb_1$) or two neoformed sets ($IIIb_2$) in a stress field characterised by σ_1, σ_3 — horizontal, σ_2 — vertical.

The following phase is linked with the activity of simple shear (Fig. 14):

Phase IV. Strike-slip faults of **system S_3**, longitudinal or diagonal, in a stress field characterised by σ_1, σ_3 — horizontal, σ_2 — vertical. Opening of fractures and mineralisation of the dextral set of **system S_1** also took place during this phase. This would point to a predominance of dextral movement along overthrusts.

Phases V and VI are linked with the post-orogenic heave of the Carpathians in a stress field characterised by σ_1 — vertical, σ_2, σ_3 — horizontal (Fig. 14).

SE–NW extension:

Phase V. Transverse normal faults from **system N_1** possibly due to local (in the SW) extension along directions parallel to the overthrusts. Locally the faults have reactivated faults of **system S_1**.

SW–NE and N–S extension:

Phase VI. Normal faults of **system N_2** and N_3, which were developed as the youngest faulting event.

REGIONAL REVIEW

The first phase of faulting is very common across the whole Polish Outer Carpathians though reverse faults formed during variable orientations of compression. For example, in the western part reverse faults originated during NNW-directed thrusting (Decker *et al.*, 1997), which lasted from the Eocene/Oligocene up to Early Miocene times. In the Romanian Carpathians in turn, the first tectonic event was characterised

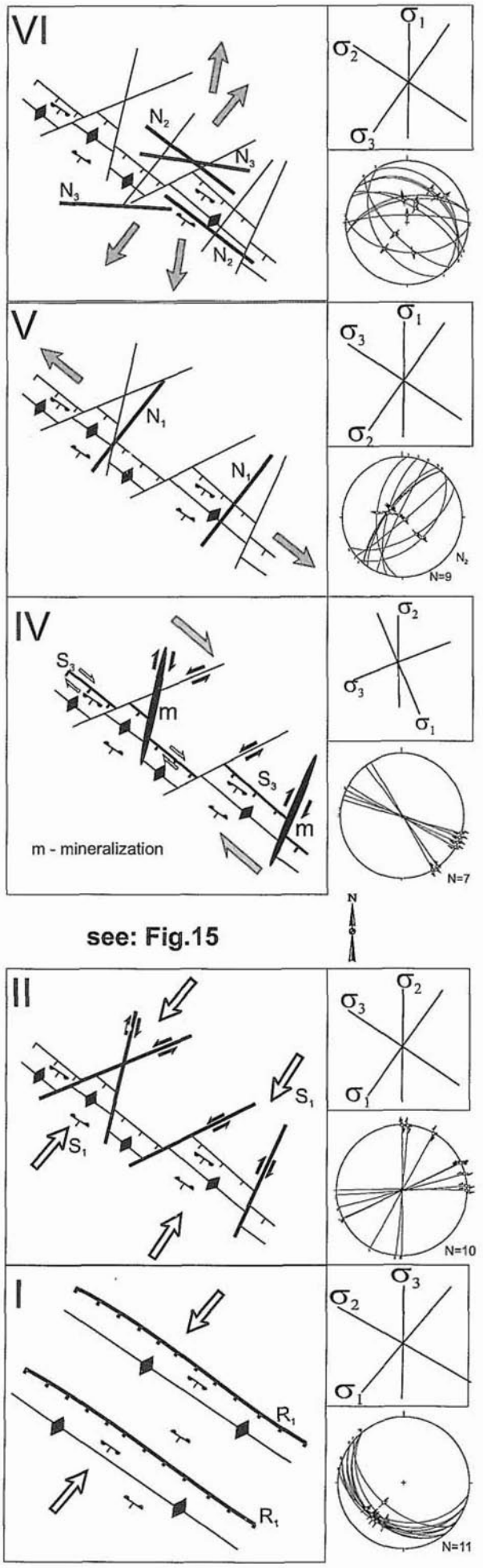

Fig. 14. Main stages of development of the fault pattern in the study area with examples of diagrams and stress regimes

Axial planes of main anticlines and overthrusts are shown; for other explanations for symbols see text

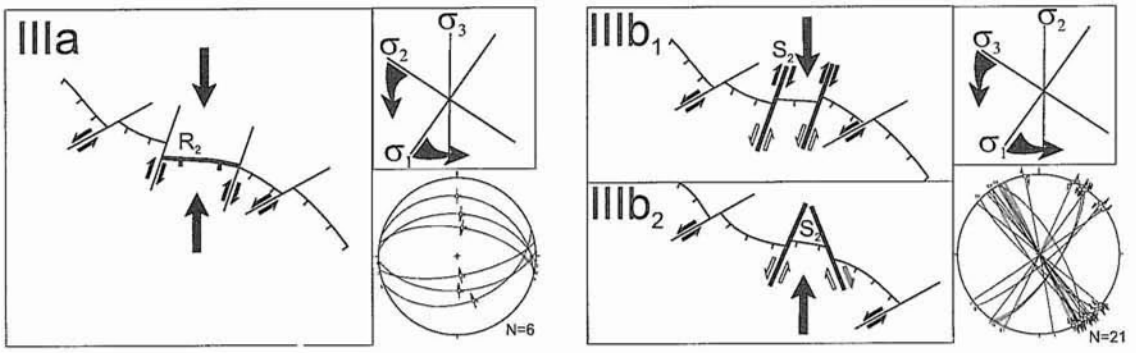

Fig. 15. Local stages of development of the fault pattern formed during N–S compression

by WSW–ENE directed shortening of Middle Miocene age (Manteo and Bertotti, 2000). In the study area reverse faults of system R_1, which formed during SW–NE compression, typical of the eastern segment of the Polish and probably Ukrainian Outer Carpathians, occur. They were probably formed in Early to Middle Miocene times.

Development of conjugate strike-slip faults, similar to those from the second phase, was also observed in the whole arc of the Polish Carpathians and postdates the formation of reverse and thrust faults. These were also formed during compression, the direction of which varies from SSE–NNW in the west, through N–S in the central part, to SW–NE in the east of the Polish Outer Carpathians. Similar strike-slip faults were observed in the Romanian Carpathians, though they originated during a NNE–SSW compressional event in Late Miocene-Early Pliocene times (Manteo and Bertotti, 2000), so the compression in the area investigated took place probably between the Middle and Late Miocene.

Observed dextral strike-slip movements along pre-existing thrust planes were noted only in the eastern part of the Outer Carpathians (to the east of Poprad river) and within inner parts of the orogen. On the other hand, in the western part, sinistral movements prevail. Such architecture suggests thrusting of the central part of the Polish Outer Carpathians northwards. This could have taken place during post-Middle Miocene times (Decker *et al.*, 1999).

Extensional phases are the most problematic, differing in evolution in particular parts of the Carpathians. They could indicate areas with smaller or larger amplitudes of post orogenic heave.

Acknowledgements. The author wishes to express his gratitude to Dr. hab. Antoni Tokarski and Dr. Kurt Decker for facilitating his acquaintance with methods of fault analysis, to Prof. Dr. hab. Leonard Mastella for fruitful discussions, and to Dr. Antoni Wójcik and Dr. Marek Jarosiński for critical reviewes.

REFERENCES

ALEKSANDROWSKI P. (1985) — Graphical determination of principal stress directions for slickenside lineation population: an attempt to modify Arthaud's method. J. Structur. Geol., **7**: 73–82.

ALEKSANDROWSKI P. (1989) — Structural geology of the Magura Nappe in the Mt. Babia Góra region, western Outer Carpathians (in Polish with English summary). Stud. Geol. Pol., **96**.

ANDERSON E. M. (1951) — The dynamics of faulting — 83 S. Oliver and Boyd. London

ANGELIER J. (1979) — Determination of the mean principal directions of stress for a given fault population. Tectonophysics, **56**:17–26.

ANGELIER J. (1994) — Fault slip analysis and paleostress reconstruction. In: Continental Deformation (ed. P. L. Hancock): 53–100. Pergamon Press. Cambridge.

ANGELIER J. and GOUGEL J. (1979) — Sur une methode simple de determination des axes principaux des contraintes pour une population de failles. C.R. Acad. Sc. Paris, **288**: 307–310.

ARTHAUD F. (1969) — Methode de determination graphique des directions de raccourcissement, d'allongement et intermediaire d'une population de filles. Bull. Soc. Geol. France, **11**: 729–737.

DADLEZ R. and JAROSZEWSKI W. (1994) — Tektonika. PWN. Warszawa.

DECKER K., NEŚCIERUK P., REITER F., RUBINKIEWICZ J., RYŁKO W. and TOKARSKI A. K. (1997) — Heteroaxial shortening, strike-slip faulting and displacement transfer in the Polish Carpathians. Prz. Geol., **45** (10/2): 1070–1071.

DECKER K., TOKARSKI A. K., JANKOWSKI L., KOPCIOWSKI R., NEŚCIERUK P., RAUCH M., REITER F. and ŚWIERCZEWSKA A. (1999) — 5th Carpathian Tectonic Workshop. Materiały konferencji terenowej.

ETCHECOPR A. *et al.* (1981) — An inverse problem in microtectonics for the determination of stress tensors from fault striation analysis. J. Structur. Geol., **3**: 51–65.

GRUSZCZYŃSKI M. and MASTELLA L. (1986) — Calcareous tufas in the area of the Mszana Dolna tectonic window (in Polish with English summary). Ann. Soc. Geol. Pol., **56** (1/2): 117–132.

GUCIK S., PAUL Z., ŚLĄCZKA A. and ŻYTKO K. (1980) — Mapa geologiczna Polski, 1:200,000, B, sheet Przemyśl, Kalników. Inst. Geol. Warszawa.

HANCOCK P. L. (1985) — Brittle microtectonics: principles and practice. J. Structur. Geol., **7**: 437–457.

JAROSZEWSKI W. (1968) — Curved fault striae and the mechanism of faulting (in Polish with English summary). Acta Geol. Pol., **18** (1): 233–240.

JAROSZEWSKI W. (1980) — Tektonika uskoków i fałdów. Wyd. Geol. Warszawa.

JAROSZEWSKI W. (1984) — Fault and Fold Tectonics. PWN. Warszawa.

KSIĄŻKIEWICZ M. (1972) — Budowa geologiczna Polski, **4**, Tektonika, part 3, Karpaty. Inst. Geol. Warszawa.

LISLE R. J. (1987) — Principal stress orientation from faults: an additional constraint. Ann. Tecton., **1** (2): 155–158.

MANTEO L. and BERTOTTI G. (2000) — Tertiary tectonic evolution of the external East Carpathians (Romania). Tectonophysics, **316**: 255–286.

MASTELLA L. (1988) — Structure and evolution of Mszana Dolna tectonic window, Outer Carpathians, Poland (in Polish with English summary). Ann. Soc. Geol. Pol., **58** (1–2): 53–173.

MASTELLA L. and SZYNKARUK E. (1999) — Analysis of the fault pattern in selected areas of the Polish Outer Carpathians. Geol. Quart., **42** (3): 263–276.

OPOLSKI Z. (1930) — Esquisse de la tectonique des Karpates entre Osława–Łupków et Użok–Sianki (in Polish with French summary). Spraw. Państw. Inst. Geol., **5** (3/4): 617–658.

PETIT J. P. (1987) — Criteria for sense of movement on fault surfaces in brittle rocks. J. Structur. Geol., **9** (5–6): 597–608.

RECHES Z. (1983) — Faulting of rocks in three dimensional strain fields — II. Theoretical analysis. Tectonophysics, **95**: 133–156.

RECHES Z. (1987) — Determination of the tectonic stress tensor from slip along faults that obey the Coulomb yield condition. Tectonics, **6**: 849–861.

REITER F. and ACS P. (1999) — TectonicsFP: computer software for structural analysis. Licence nr 1.5-9901-HLC.

RUBINKIEWICZ J. (1998) — Development of joints in Silesian nappe (Western Bieszczady, Carpathians, SE Poland) (in Polish with English summary). Prz. Geol., **46** (9): 820–826.

RUBINKIEWICZ J. (1999) — Mapa geologiczna płaszczowiny śląskiej pomiędzy Osławą a Hoczewką w Bieszczadach w skali 1:25,000. Arch. IGP UW. Warszawa.

SPANG J. H. (1972) — Numerical method for dynamic analysis of calcite twin lamellae. Geol. Soc. Am. Bull., **83** (1): 467–472, 6 figs., 1 tab.

SPERNER B. and RATSCHBACHER L. (1993) — Fault-striae analysis: a turbo pascal program package for graphical presentation and reduced stress-tensor calculation. Computers and Geosciences, **19** (9): 1361–1388.

ŚLĄCZKA A. (1968) — Objaśnienia do Szczegółowej Mapy Geologicznej Polski, 1:50,000, sheet Bukowsko. Inst. Geol. Warszawa.

ŚLĄCZKA A. (1996) — Oil and gas in the northern Carpathians. In: Oil and Gas in the Alpidic Thrustbelts and basins of Central and Eastern Europe (eds. G. Wessely and W. Liebl). EAPG Spec. Publ., **5**, 187–195.

TOŁWIŃSKI K. (1933) — Centralna depresja karpacka. Geol. Statyst. Naft., **7**: 362–366.

TURNER F. J. (1953) — Nature and dynamic interpretation of deformation lamellae in calcite of three marbles. Am. J. Sc., **251**: 276–298.

WDOWIARZ S. (1980) — The geological structure of the Central Carpathian Synclinorium in the Rajskie–Zachoczewie (in Polish with English summary). Biul. Inst. Geol., **326**: 5–24.

WDOWIARZ S. (1985) — On some aspects of geological structure and oil and gas accumulation of the Central Carpathian Synclinorium in Poland (in Polish with English summary). Biul. Inst. Geol., **350**: 5–45.